Multicomponent AVO analysis of a single thinning bed

Jessie M Arthur* and Don C Lawton

ABSTRACT

Synthetic seismograms are constructed with Ricker wavelets of 30 Hz and 50 Hz dominant frequency to represent a gradually thinning bed with equal magnitude and opposite polarity reflection coefficients in a homogeneous medium. A tuning thickness of λ/4 is observed for both the PP and PS synthetic data. AVO intercept and gradient crossplot analysis for a slow velocity, less density thin layer are compared with a fast velocity and higher density layer. For a slow velocity thin layer above tuning thickness, the AVO crossplot results show a counter-clockwise rotation, indicating a negative correlation as the gradient decreases and the reflection coefficient magnitude increases. For the fast velocity thin layer, a clockwise rotation occurs in the AVO crossplot results as the bed thins. The gradient increases and the reflection coefficient magnitude decreases. Results below tuning thickness behave non-linearly and are less predictable.

INTRODUCTION

Thin bed reflection studies are important to evaluate resources in thin reservoirs, studying sedimentary processes, and interface resolution for structure mapping. Resolving and defining thin layers is difficult and challenging (Chang et al., 1996), and many approaches can be taken. Vertical seismic resolution is defined by Widess (1973) as the thickness equal to one eighth of the predominant seismic wavelength. However, this threshold does not account for noise and wavelet broadening, so one quarter of the predominant wavelength is taken as an industry standard for thin bed vertical resolution. This vertical resolution threshold is also known as the tuning thickness, or tuning point, and is where maximum constructive amplitude occurs.

Some examples of literature which studied the amplitude of thin beds where the upper and lower interfaces have equal and opposite polarity include: Widess (1973), Chung and Lawton (1990), Chang et al. (1996), and Liu and Schmitt (2003). Widess (1973) defines a thin bed whose thickness d, is less than 1/8th of the dominant seismic wavelength λ, since at this thickness the reflected wavelet resembles the derivative of the convolved zero-phase source wavelet and a thin layer can be resolved. The simple case of a thin layer embedded in a homogeneous higher velocity medium was studied, ignoring transmission losses.

Chung and Lawton (1990) studied various two-term reflectivity series models convolved with a Ricker wavelet representing a single thin bed in a simple wedge model. The tuning thickness was found to be 1/4th the predominant wavelength. A linear trend for maximum amplitude increasing with thickness was observed for the case of equal but opposite polarity. A nonlinear trend was found for equal polarity cases.

Another approach is to focus on detecting the existence of layers rather than resolving thin layer reflections as taken by Chang et al. (1996). In their study, a synthetic seismogram is generated using a zero-phase Ricker wavelet convolved with spikes of

equal amplitude and opposite polarity. A Hilbert transform is used to detect reflectivity strength and amplitude for layers less than 1/8th dominant wavelength.

Liu and Schmitt (2003) investigated the amplitude variations with offset (AVO) response with angle of incidence of a thin bed with opposite polarity pre- and post-critical reflections. They define the thickness of an ultra thin layer to be less than one quarter the dominant wavelength. This study differs from the previous studies, which apply only to normal incidence reflections using ray theory.

AVO analysis is useful in indentifying lithology, predicting pore fluid content, and evaluating hydrocarbon potential. The AVO effect is dependent on the petrophysical properties V_P, V_S, and density p (Veeken and Davies, 2006). Crossplot analysis of AVO parameters such as a scatter plot of P-wave reflectivity (intercept) and the AVO gradient defined by Shuey's approximation of the Zoeppritz equations are useful in identifying linear trends in clusters of data for further analysis. The Zoeppritz equations describe the angular dependence of reflection coefficients for plane waves and are the basis of AVO analysis. The Zoeppritz approximations are discussed later in further detail.

This study examines the case of thinning beds having equal magnitude and opposite polarity. Two geological models are investigated; a gradually thinning embedded lower velocity and density layer, and a gradually thinning embedded higher velocity and density layer in homogeneous media. Models of flat reflectors are created with a moderate acoustic contrast at the interfaces. AVO crossplot analysis investigates the reflectivity behaviour of thinning beds with offset.

MODEL PARAMETERS

To examine the response of a single thin bed, two geologic models are considered. Both models represent a two-term reflectivity series of opposite polarity and equal strength. The geologic parameters are given in Table 1. Geologic model I represents a thick homogeneous sandstone unit with a single thin shale bed at 1000 m depth of varying thicknesses that gradually thin from the bottom. Geologic model II represents the opposite case, a higher velocity sandstone layer embedded in a homogeneous shale unit.

Table 1. Geologic models used to investigate the response of a thinning bed.

	Unit	P-wave (m/s)	Density (kg/m^3)	S-wave (m/s)
Model I	Sandstone 1	3000	2650	1670
	Shale	2500	2200	1250
	Sandstone 2	3000	2650	1670
Model II	Shale 1	2500	2200	1250
	Sandstone	3000	2650	1670
	Shale 2	2500	2200	1250

The geologic models are developed in LAS (ASCII) file format well logs. Density, P-wave sonic, and S-wave sonic well logs were generated and edited in MATLAB using the CREWES toolbox functions *readlas.m* and *writelas.m*. The thin bed thicknesses vary with dominant wavelength and are therefore frequency dependent. A fine well log sample

rate of 0.25 m was selected to best represent the variations of thin layers. Thickness ranges of the thin beds, for dominant frequencies of 30 Hz and 50 Hz, are summarized in Table 2. The minimum thickness studied is approximately 5 metres.

Table 2. Thin bed thickness (metres) based on dominant frequency and varying wavelength for both geologic models. The thin bed starts at 1000 m depth. Dominant wavelength is represented by the symbol λ.

	MODEL I		MODEL II
	Thickness (m)		Thickness (m)
	f = 30 Hz	f = 50 Hz	f = 50 Hz
3λ	250	150	180
λ	83.3	50.0	60
λ/2	41.7	25.0	-
λ/3	27.8	16.7	-
λ/4	20.8	12.5	15
λ/6	13.9	8.3	-
λ/8	10.4	6.3	7.5
λ/10	8.3	5.0	3.8

   Wavelets and seismograms were constructed in the program SYNGRAM (University of Calgary, CREWES). Two zero-phase Ricker wavelets of 30 Hz and 50 Hz with 0.002 s sample rates were created (Figure 1) and convolved with the two-term reflectivity series to generate synthetic PP and PS primaries-only seismograms of trace gathers using a SEG standard polarity convention. Exact Zoeppritz equations calculate the reflection amplitudes for plane-waves normal to the boundary interface and incident angles are displayed by ray-tracing calculations. A log integration interval of 0.0005 seconds (Figure 2) was selected to create blocky logs as a smoother for ray-tracing calculations.

   Receiver geometry parameterization depended on whether a PP or PS seismogram was generated. For PP seismograms, vertical component geophones are parameterized with a 100 m spacing and 1500 m maximum offset. A maximum offset-depth ratio of 1.5 was selected. Offset-depth ratios that are too low cause restrictive apertures resulting in anomalous results (Ross, 2000). Horizontal component geophones were selected to generate PS seismograms. Normal moveout (NMO) was also removed, creating flattened gathers for further analysis.
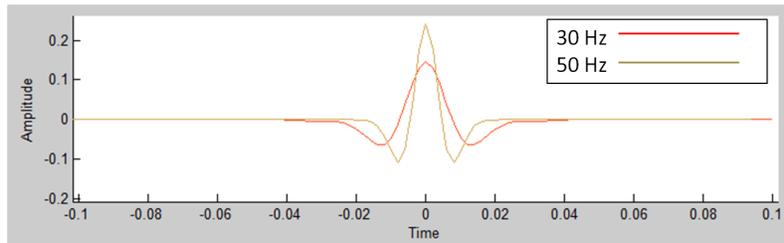
FIGURE 1. Zero-phase 30 Hz and 50 Hz Ricker wavelets created in SYNGRAM to generate seismograms.
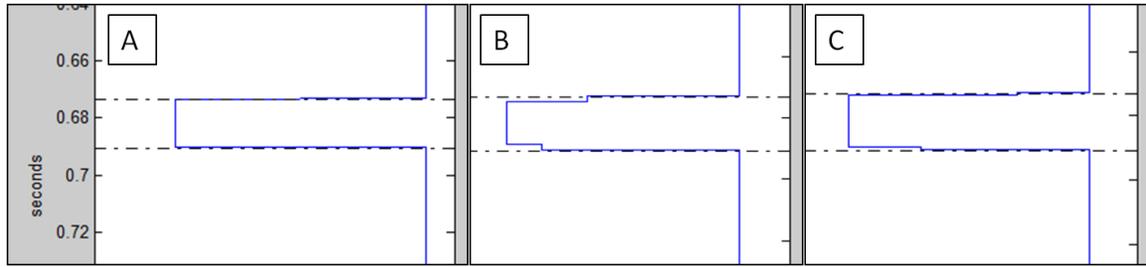
FIGURE 2. A log integration interval of 0.0005 s was selected to create a blocky log most similar to the normal log. A) Normal P-wave sonic log for λ/4 at 30 Hz dominant frequency. B) Blocky log with sample rate=0.002. C) Blocky log with sample rate=0.0005.

The parameters of geologic model I investigates 30 Hz and 50 Hz dominant frequencies for PP synthetic seismic data, and 30 Hz for PS synthetic seismic data. For additional analysis, the thin bed parameters of geologic model II use a dominant frequency of 50 Hz for PP synthetic data. AVO analysis is then carried forward with the 50 Hz dominant PP synthetic data for both models.

THE ZOEPPRITZ EQUATIONS

The Zoeppritz equations describe how the energy of a plane wave partitions into transmitted and reflected waves at an elastic interface between two isotropic and homogeneous half-spaces, relative to the incident angle. Linear approximations of the Zoeppritz equations are useful since the non-linear equations are awkward and lack physical insight for visualization (Castagna, 1993a).

Shuey (1985) simplified the Zoeppritz equations to give the P-wave reflection coefficient as a function of angle of incidence:

$$R_{PP}(\theta) = A + B \sin^2\theta + C(\tan^2\theta - \sin^2\theta) \tag{1}$$

where A represents the linearized zero-offset P-wave reflection coefficient, B is the AVO gradient which approximates reflection amplitudes at various offsets and depends on the sine of the angle of incidence squared, and C is the AVO curvature term. A positive gradient signifies that amplitude increases with offset in a crossplot of R_p versus $\sin^2\theta$ (Veeken and Davies, 2006). These coefficients are often used as AVO indicators for modelling studies (Castagna and Smith, 1994). All three terms in Equation 1 are equivalent to the Aki and Richards (1980) R_{PP} approximation between two similar half-spaces. However, Shuey's approximation assumes Vp/Vs=2, and for angle of incidence about greater than 30° the third term drops leaving a simpler two-term equation. Shuey also incorporated Poisson's ratio into the approximation.

The University of Calgary CREWES Zoeppritz Explorer applet was used to investigate how reflection coefficients change with angle of incidence given the model parameters described above for a sandstone unit with an embedded shale layer (Figure 3).

The Aki-Richards approximation is used in the applet. This approximation gives the linear dependence of reflection coefficients of elastic differences between the two layers.

The Zoeppritz equations are only capable of predicting reflection and transmission at a single interface. Figure 3 shows the predicted reflection coefficient at an interface using the modelled parameters described above. The first interface of model I, with sandstone as the top layer and a lower velocity and density shale as the bottom layer is shown in Figure 3a. The reflection coefficient magnitude increases slightly from -0.2 to -0.1, then reaches an inflection point at 50° where the reflection coefficient becomes more negative with increasing angle of incidence. Figure 3b represents the first interface of model II, with a shale top layer and a higher velocity and density sandstone bottom layer. The critical angle of incidence is reached at 56° where the refracted wave travels along the interface.
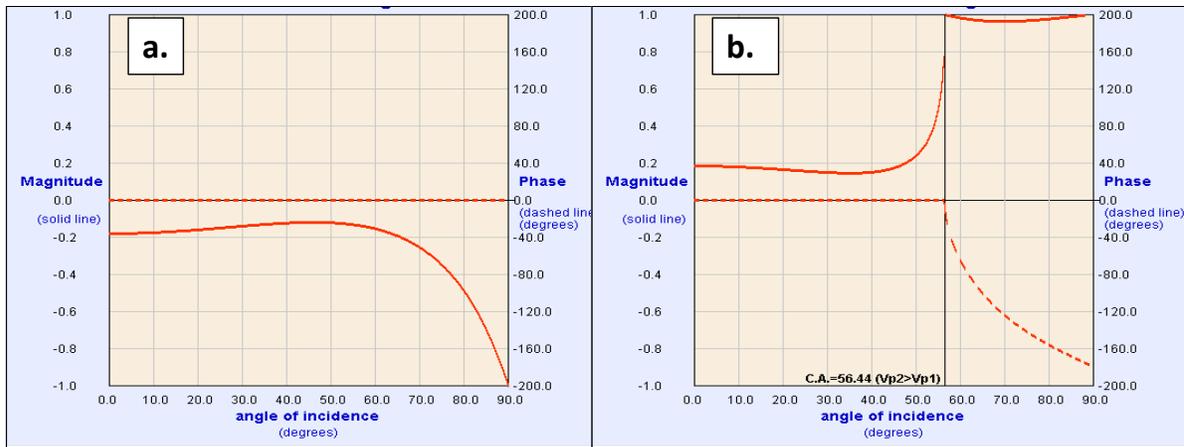
FIGURE 3. P-wave reflection coefficient compared to angle of incidence from the Zoeppritz explorer applet. The solid red line is the reflection coefficient magnitude, and the dashed line represents phase in degrees. A) Parameters shown for an interface with a sandstone top layer (ρ=2650 kg/m^3, Vp=3000 m/s) and a shale bottom layer (ρ=2200 kg/m^3, Vp=2500 m/s). Reflected energy increases slightly and steadily with angle of incidence until an inflection point is reached at 50°, then suddenly becomes more negative. B) Model parameters for a top shale layer and a bottom sandstone layer. Reflected energy decreases slightly until it increases significantly to unity when the near-critical angle of incidence is reached.

Since the Zoeppritz equations can only predict the reflection and transmission coefficients at a single interface, these equations are not suitable to study the amplitude and AVO response of a thin bed problem (Liu and Schmitt, 2003).

It is also noted that SYNGRAM generates primaries-only seismograms using the exact Zoeppritz equations. Simmons and Bacchus (1994) modelled the AVO response of thin beds, and showed that primaries-only modelling does not accurately model the true seismic response of a thin bed. The study showed results where primaries-only Zoeppritz modeling increased in AVO as the bed becomes thinner, which was deemed as physically illogical. A linearized Zoeppritz approximation would show decreasing amplitudes with offsets, which better represents a true solution. Other modes of propagation, such as converted shear waves, should also be included to best represent reflection modelling.

SYNGRAM SEISMOGRAM RESULTS

Model I: PP-Reflection Data

PP-reflection synthetic seismograms with a thin shale layer embedded in sandstone were created with both a zero-phase 30 Hz wavelet and then a 50 Hz wavelet (Figure 4), and the results are compared. For each of the two datasets, the thinnest layer modelled was approximately 5 metres. A positive amplitude peak indicates a P-wave impedance increase.

For both the 30 Hz and 50 Hz seismogram sets, a distinguishable trough at the shale interface and peak at the second sandstone interface of equal and opposite polarity is apparent until thickness of half wavelength ($\lambda/2$). However when thickness is approximate to the tuning thickness $\lambda/4$, the signal from the two interfaces converges and interference occurs. As the shale bed thins below tuning thickness, amplitudes vary slightly with further convergence of the top and bottom shale reflections, which are no longer distinguishable as separate interfaces. Maximum angle of incidence occurs at 37° for 1500 metre offset.

Model I: PS-Reflection Data

To compare the tuning thickness and results from the PP-reflection data, PS-reflection synthetic seismograms with a thin shale layer embedded in sandstone were also created with a zero-phase 30 Hz Ricker wavelet and shown in Figure 5. The PS data shows near zero reflection coefficients at near offsets and normal incidence. Amplitude is shown to increase with offset. Incident angles have increased in the PS data to 40 degrees for offsets of 1500 metres.

The PS reflection data shows the top and bottom shale interface as a separate trough and peak of equal and opposite polarity at thickness $\lambda/4$ that is better resolved than the 50 Hz PP data. This is a result of tuning effects being less severe for PS wave maximum peak amplitude (Chung and Lawton, 1991).
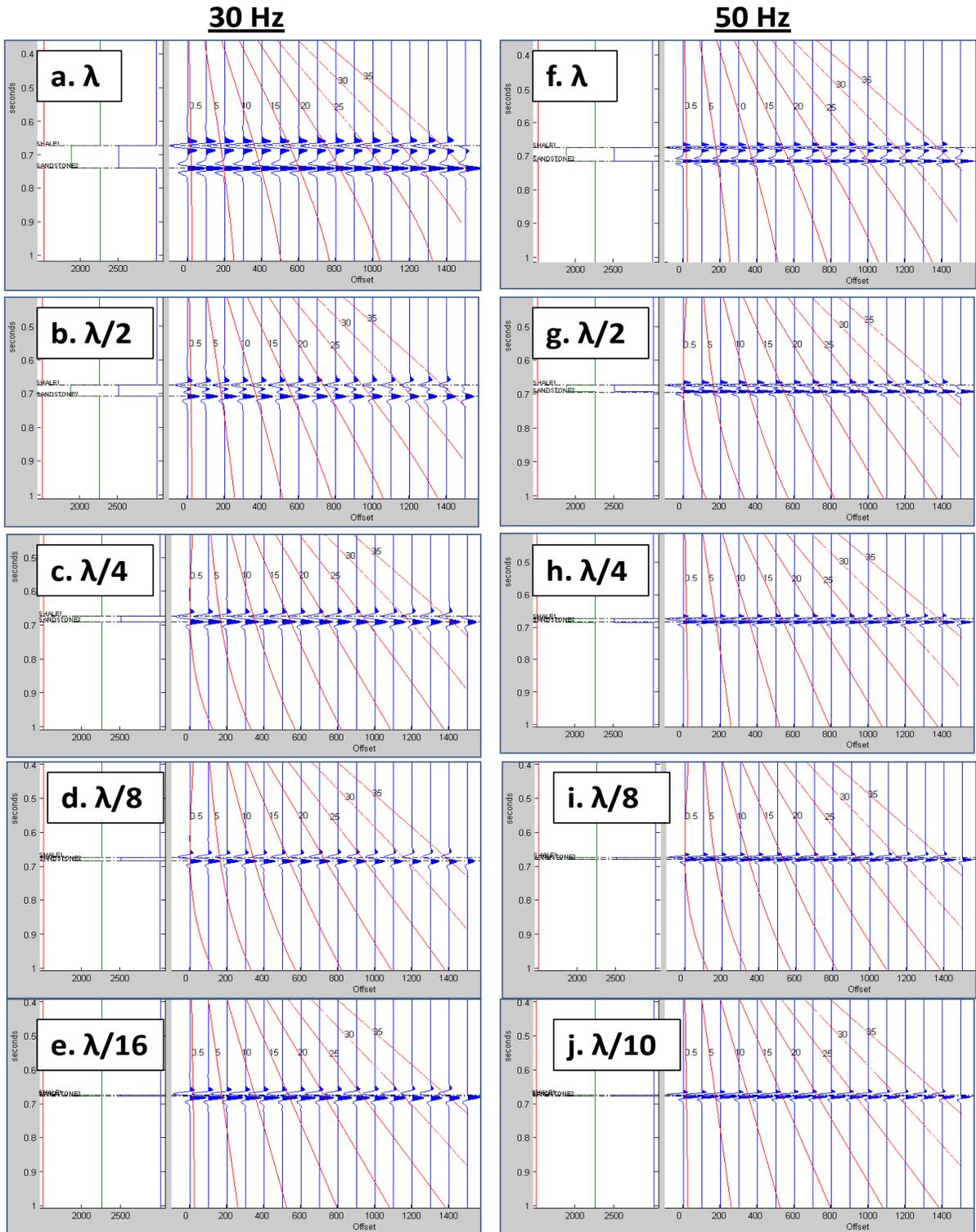
FIGURE 4. The boundary effects of a thin layer are observed to affect the seismogram wavelets. A-E: PP Synthetic seismograms created with a zero-phase 30 Hz Ricker wavelet, F-J: PP Synthetic seismograms created with a zero-phase 50 Hz Ricker wavelet. Angle of incidence is shown in degrees on the seismograms. Logs plotted are Vs (red), RHO (green), and Vp (blue) on the left of each image. Tuning thickness for both seismograms occurs at λ/4.
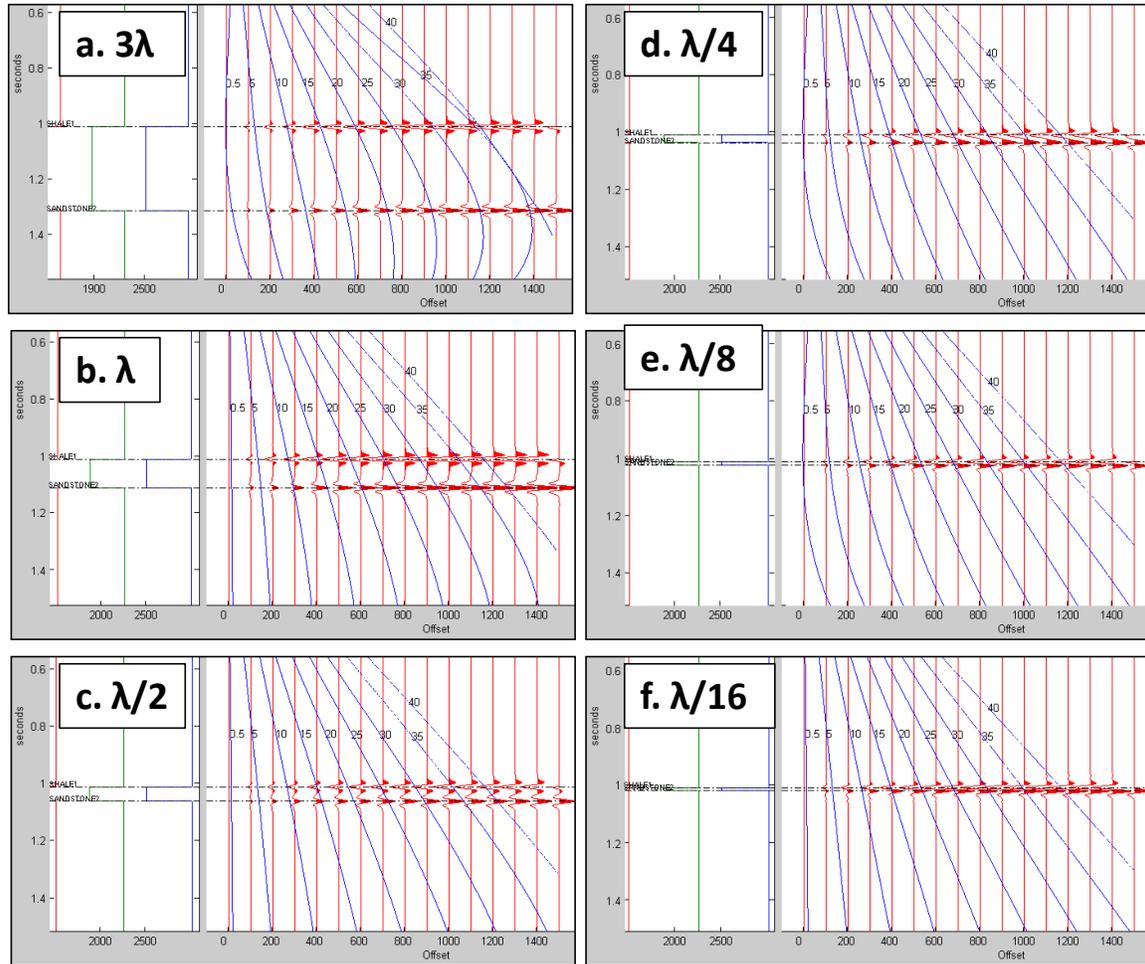
FIGURE 5. PS Synthetic seismograms created with a zero-phase 30 Hz Ricker wavelet. Angle of incidence is shown in degrees on the seismograms, with maximum angle at 40°. Logs plotted are Vs (red), RHO (green), and Vp (blue) on the left of each image. The SEG standard used indicates positive amplitude for an S-wave impedance increase. In contrast to the PP data, tuning will not occur at λ/4 exactly, as tuning effects are less severe for PS wave maximum amplitude.

Model II: PP-Reflection Data

PP-reflection synthetic seismograms with a higher velocity and density sandstone layer embedded in a thick homogeneous shale unit are created with a zero-phase 50 Hz wavelet (Figure 6). Modelled layers range from 5 to 50 metres in thickness. For the first shale-sandstone interface, a positive amplitude peak indicates a P-wave impedance increase. The impedance decreases as the raypaths cross the second interface and results in a trough. The tuning thickness is in agreement with Model I and occurs at λ/4, where the two events become unresolvable. Amplitude is also observed to decrease slightly with increasing offset.
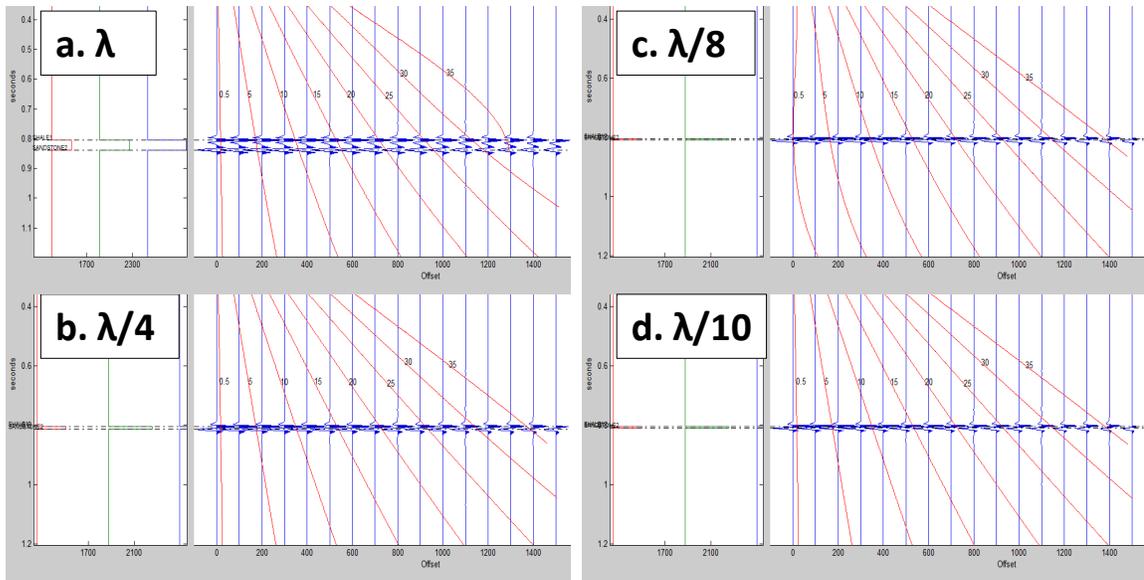
FIGURE 6. The boundary effects of a thin sandstone layer embedded in shale.. A-D: PP Synthetic seismograms created with a zero-phase 50 Hz Ricker wavelet for geologic model II. Angle of incidence is shown in degrees on the seismograms. Logs plotted are Vs (red), RHO (green), and Vp (blue) on the left of each image.

AVO CROSSPLOT ANALYSIS

Geologic model I

The Hampson-Russell software module AVO was used to analyze the SYNGRAM generated 50 Hz PP-synthetic gathers and wells, then apply AVO analysis on the 2D data. Figure 7 shows bed thicknesses ranging from λ to $\lambda/10$. The leftmost column shows the trough and peak selected for AVO analysis on the seismogram with guidance from the well log. The trough occurs on the top of the sandstone-shale interface, and the peak on the bottom shale-sandstone interface. The vertical resolution becomes complicated at the tuning thickness of $\lambda/4$, where due to interference, it becomes difficult to analyze the individual top and bottom interfaces of the thin shale bed.

The center column shows amplitude variation with offset as the shale bed becomes thinner. The results show similar and symmetrical behaviour for the top and bottom interface of thinning beds. In the modelled synthetic dataset, the theoretical Zoeppritz critical angle of approximately 50° is not reached. Once at tuning thickness, the separate interfaces are lost and it is difficult to select the peak and trough corresponding to the well log as the wavelets begins to interfere. The maximum amplitudes remain consistent as the layer thins; however, the minimum amplitude begins to diminish at minimum offsets. At the tuning thickness, the separate interfaces constructively interfere and the Zoeppritz equations are no longer suitable for thin beds as they can only predict reflection coefficients at a single interface.

Figure 7 displays gradient analysis based on time pick pairs of the first event, a trough; and the second event, a peak. The first column shows PP-reflection seismograms of

various thicknesses. The red line across the trough is the time pick for the first sandstone-shale interface, and the blue line across the peak is the time pick for the bottom shale-sandstone interface. The middle column is an offset-amplitude crossplot, showing decreasing amplitude with offset. The rightmost column displays an Intercept-Gradient crossplot analysis. A linear trend is drawn between intercept-gradient points based on the trough and peak time picks. Other various A-B pairs shown as various points across the crossplot represent other time picks events.

A composite of the intercept versus gradient crossplot results is shown in Figure 8. The time pick points from the trough fall into quadrant II, and the points from the peak time pick fall into quadrant IV. As the bed thins from 3λ to the tuning thickness of $\lambda/4$, the background trend in the Intercept-Gradient crossplot rotates counter-clockwise and the slope increases from -0.94 to -0.78. As the bed continues to thin past tuning thickness, the results become more unstable and anomalous. A separate data cluster of the time-pair picks forms and could be misinterpreted as an AVO anomaly.

In summary, the results follow a counter-clockwise rotational trend of decreasing gradient above tuning thickness, and therefore amplitude decreases with offset. However, once tuning thickness is reached, the results become unstable as the gradient slope rotates clockwise as the bed thins below tuning.
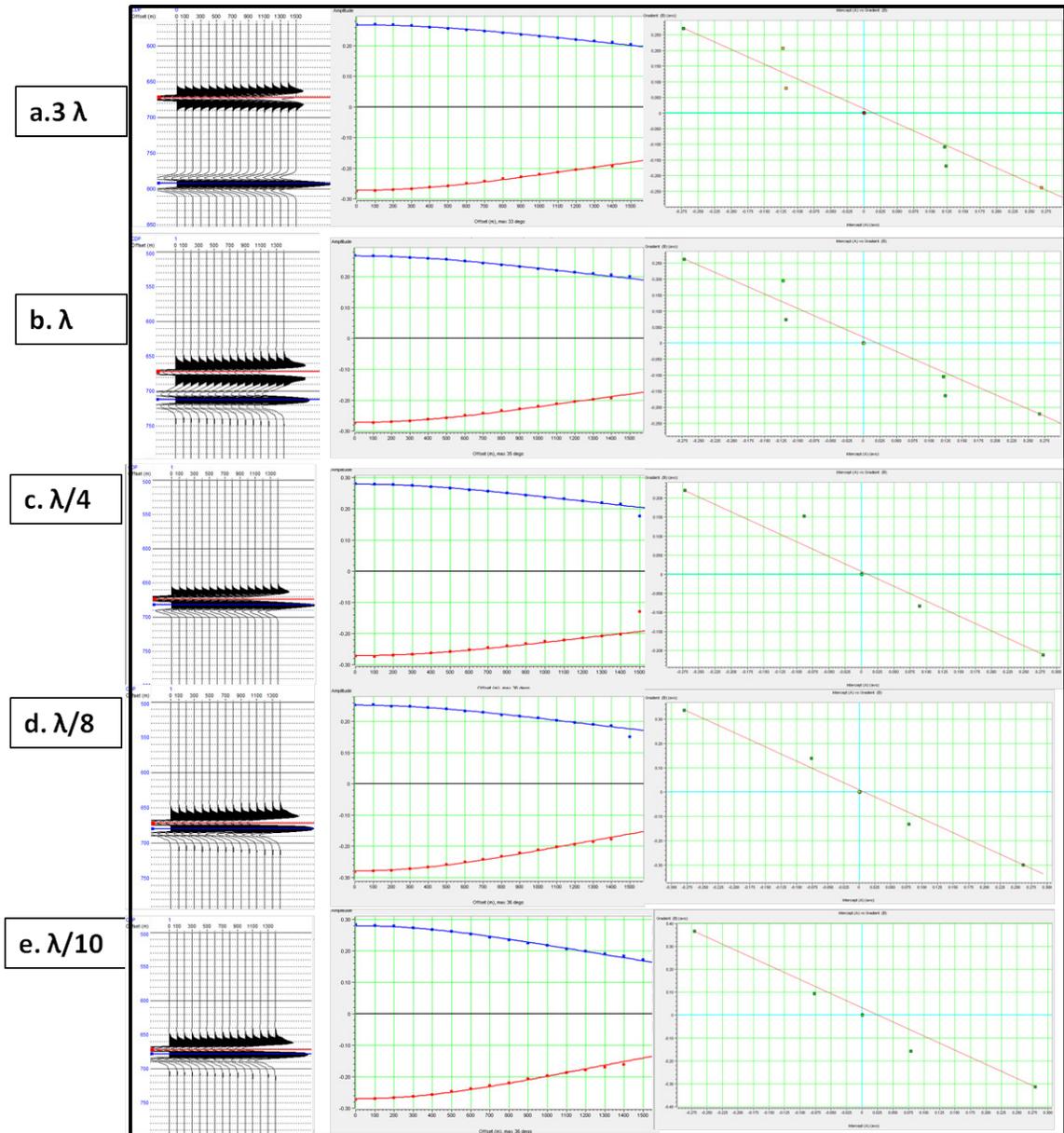
FIGURE 7. (From Left to Right) AVO analysis showing PP-reflection seismograms of various thicknesses for model I. Time picks are made on a trough and peak for changes in geologic interfaces; Offset-Amplitude crossplot showing amplitude decreasing with offset; and Intercept-Gradient crossplot for thin bed thicknesses represented by various wavelengths. A linear trend is drawn between intercept-gradient points based on the trough and peak time picks. Other various A-B pairs shown as various points across the crossplot represent other time picks events. Note at tuning thickness λ/4 and smaller, it is difficult to resolve the thin bed interfaces.
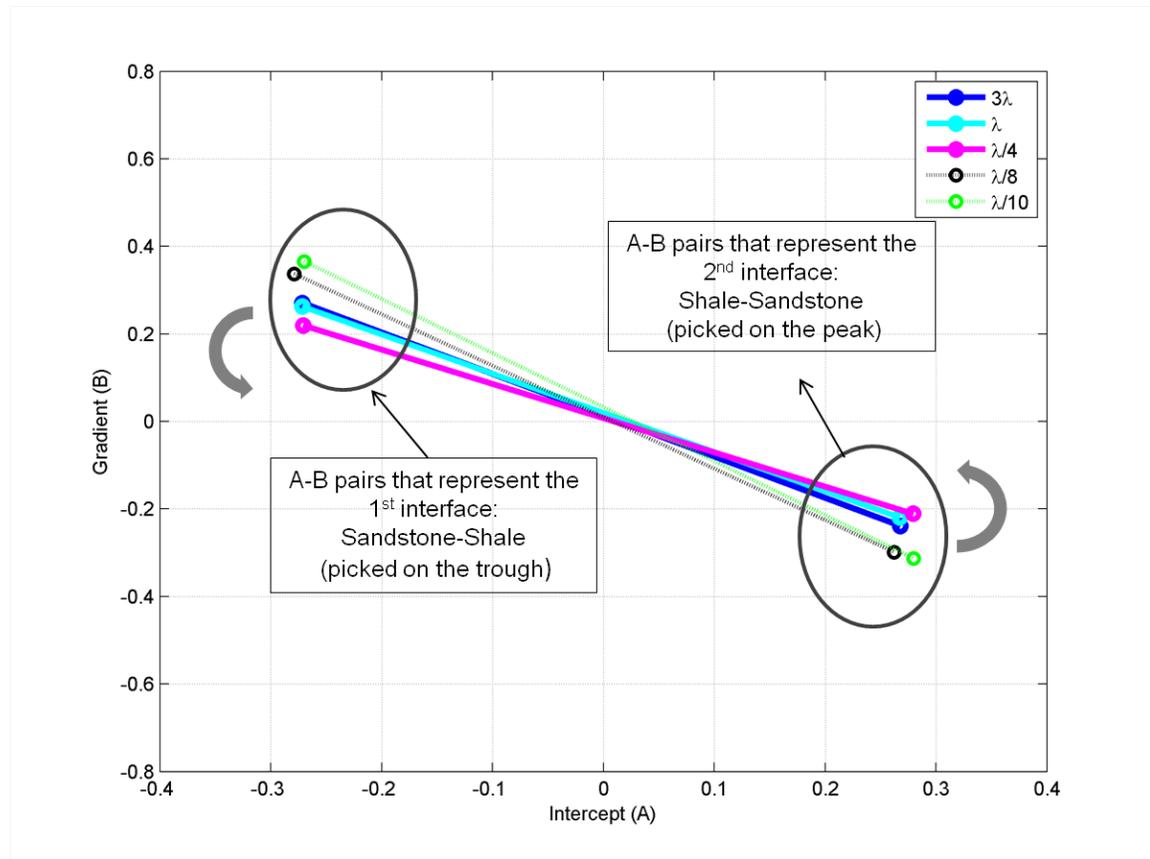
FIGURE 8. Intercept-Gradient cross-plot for Model I. The trend rotates counter-clockwise as bed thickness decreases from 3λ (slope = -0.94) until tuning thickness of λ/4 (slope = -0.78) is reached. As the bed continues to thin past tuning thickness, the results are less predictable and the slope rotates clockwise from λ/8 to λ/10 with an increasing negative gradient.

Geologic model II

The AVO results of the high velocity sandwich model are shown in Figure 9 for bed thicknesses ranging from 3λ to λ/10. An amplitude peak occurs on the top of the shale-sandstone interface, and a trough on the bottom sandstone-shale interface. As shown previously, for tuning thickness less than λ/4, the thin bed interfaces are difficult to pick due to wavelet interference.

As the sandstone bed becomes thinner, the Intercept-Gradient crossplot trend rotates clockwise and amplitude decreases with minimum offsets. Although not as apparent as in Model 1, the results below tuning thickness show variations in the AVO results (Figure 10).

Ross (2000) found that reservoir thickness variations complicate the AVO crossplot response, where the intercept-gradient response is more balanced above tuning, but below tuning the intercept variation is more dominant. Castagna (1993b) also indicates that

tuning and interference can lead to problems in AVO analysis; however the strongest aspect of AVO analysis is comparing anomalous behaviour to a background trend.
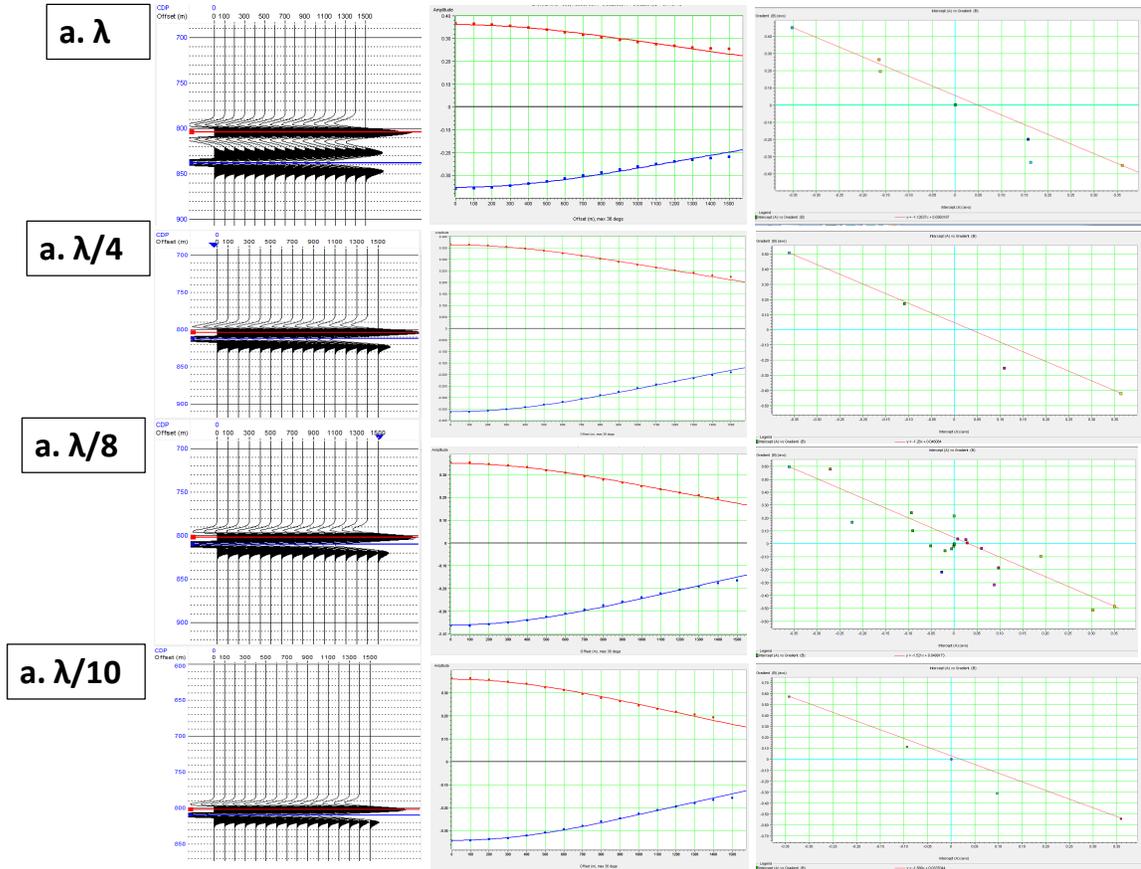
FIGURE 9. (From Left to Right) AVO analysis showing PP-reflection seismograms of various thicknesses for Model II. Time picks are made on a peak (red line) and trough (blue line) for changes in geologic interfaces; Offset-Amplitude crossplot showing amplitude decreasing with offset; and Intercept-Gradient crossplot for thin bed thicknesses represented by various wavelengths. A linear trend is drawn between intercept-gradient points based on the peak and trough time picks. Other various A-B pairs shown as various points across the crossplot represent other time picks events.
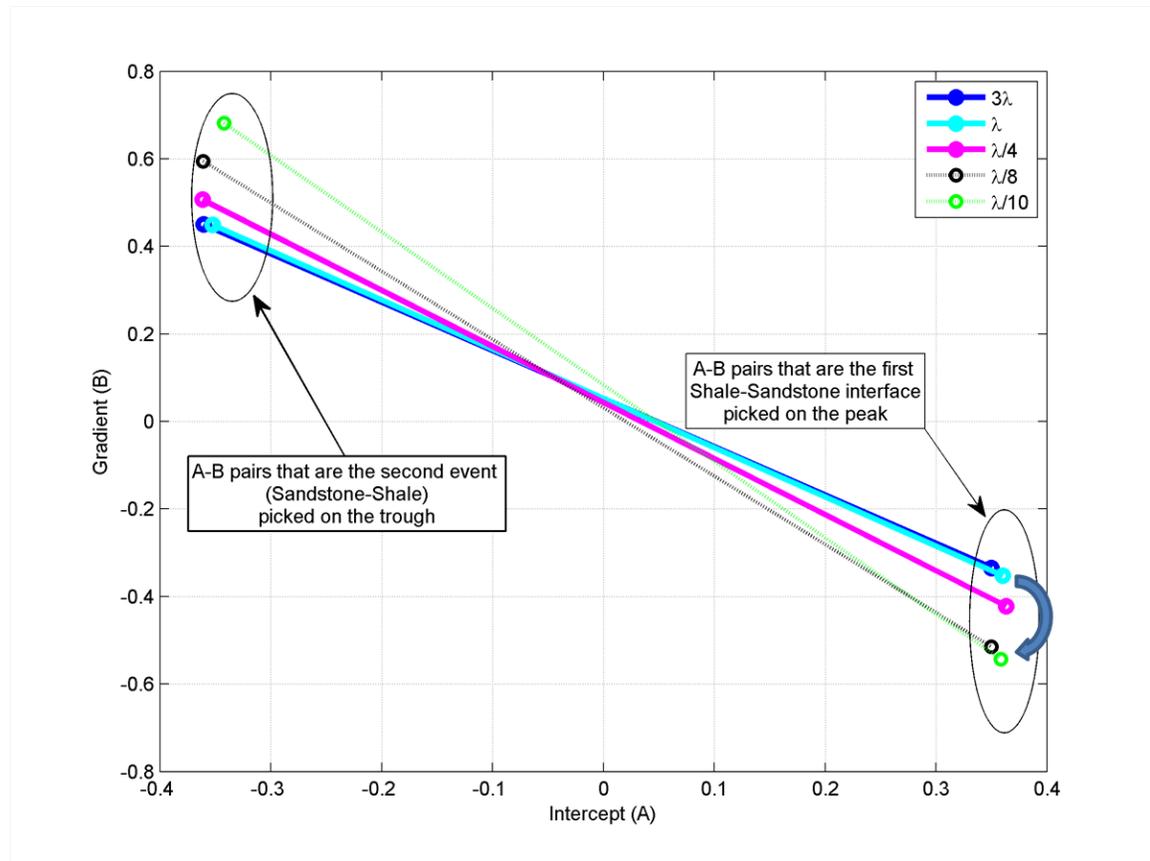
FIGURE 10. Intercept-Gradient cross-plot for Model II. The trend rotates clockwise as bed thickness decreases to tuning thickness of λ/4. As the bed continues to thin past tuning thickness, the results are less predictable and greater variation is seen with intercept in quadrants II and IV.

CONCLUSIONS

Two simple cases of each a slow and fast velocity thin layer embedded in a homogeneous medium is modelled as a synthetic seismogram with equal magnitude but opposite polarity. Thin beds below tuning thickness cause limitations and complexities in the theoretical analysis of the Zoeppritz reflection coefficients and AVO crossplot analysis as the top and bottom interfaces of the thin layer converge. Variations in the AVO crossplot due to tuning thickness can be misinterpreted as either a change in porosity or lithology. It should be noted that the tuning thickness for these modelled data are not unique, as the data can be investigated with any frequency.

Future work includes investigating thinning beds with unequal polarity models, and multiple beds. Also, by further investigating frequency and enhancing the spectral bandwidth of the seismic data, the theoretical limits of resolution can be improved and tuning thickness further decreased (Chopra et al., 2006). Using a 90 degree Ricker wavelet is proposed by Zeng (2009) to focus more on resolving the bed itself, rather than the interfaces to identify thickness. And finally, AVO modeling using a wave equation based approach rather than the Zoeppritz ray trace based approach is recommended to incorporate multiples and converted wave responses (Ross, 2000). These methods can effectively portray better realistic models for further AVO analysis.

ACKOWLEDGEDGEMENTS

REFERENCES

Aki, K., and Richards, P.G., 1980, Quantitative Seismology: Theory and methods, Vol 1, pg 153: W.H. Freeman and Co., USA.

Castagna, J.P., 1993a, AVO Analysis – Tutorial and Review, *in* Castagna, J.P., and Backus, M.M., Eds, Offset-dependent reflectivity – Theory and practice of AVO analysis: Soc. Explr. Geophysics, 3-36.

Castagna, J.P., 1993b, Petrophysical imaging using AVO: The Leading Edge, March 1993.

Castagna, J.P., and Smith, S.W., 1994, Comparison of AVO indicators: A modelling study: Geophysics, 59, 12, 1849-1855.

Chang, C.H., Shih, R.C., Chang, Y.F., 1996, Characteristics of reflectivity strength on a thin bed: TAO, 7, 3, 269-276.

Chopra, S., Castagna, J., Portniaguine, O., 2006, Seismic resolution and thin-bed reflectivity inversion: CSEG Recorder, January 2006.

Chung, H., and Lawton, D., 1990, Some properties of thin beds, CREWES Research Report.

Chung, H., and Lawton, D., 1991, Offset-dependent tuning effects of thin layers and a model. study of two layers, CREWES Research Report.

Liu, Y., and Schmitt, D.R., 2003, Amplitude and AVO responses of a single thin bed: Geophysics, 68, 4, 1161-1168.

Ross, C.P., 2000, Effective AVO crossplot modelling: A tutorial: Geophysics, 65, 3, 700-711.

Simmons, J.L., and Backus, M.M., 1994, AVO modelling and the locally converted shear wave: Geophysics, 59, 9, 1237-1248.

Shuey, R.T., 1985, A simplification of the Zoeppritz equations: Geophysics, 50, 4, 609-614.

Simm, R., 2000, The anatomy of AVO crossplots: TLE, February 2000, 150-155.

Veeken, P., and Rauch-Davies, M., 2006, AVO attribute analysis and seismic reservoir characterization: First Break, 24, 41-52.

Widess, M.B., 1973, How thin is a thin bed?: Geophysics, 38, 1176-1180.

Zeng, H., 2009, How thin is a thin bed? An alternative perspective: TLE, October 2009, 1192-1197.